Adhesion of Blended Polymer Films

Christopher Staszel[1], Suman Sinha-Ray[1], Alexander L. Yarin[1], Behnam Pourdeyhimi[2]

[1]Department of Mechanical and Industrial Engineering,

University of Illinois at Chicago,

842 W. Taylor St., Chicago, IL 60607-7022, United States

[2]3427 The Nonwovens Institute, Box 8301,

North Carolina State University

Raleigh, NC 27695-8301, United States

* Correspondence should be addressed to E-mail: ayarin@uic.edu. Phone: +1(312) 996-3472. Fax: +1(312) 413-0447.

.

1. Introduction

Polymer adhesion was previously studied in the framework of polymer physics, materials science, and technological applications [1-7]. Adhesion is a physical process of joining separate material surfaces together by means of quantum-mechanical, mechanical, chemical, or thermodynamic forces. This process is affected by polymer miscibility, and polymer blends with few exceptions tend to separate [1-7]. Accordingly, a rare miscibility or frequent immiscibility of polymers have a significant effect on the adhesive strength at the contact surfaces [1-7], typically causing a weak adhesion between two polymer surfaces. Note that several theoretical results on polymer-polymer adhesion linking it to polymer reptation through the interface is available, most notably [8-12].

Even with such weak adhesion, blended polymer systems are frequently employed for various technological applications ranging from the semi-conductor industry to the textile industry. In the semi-conductor industry, a process known as spin-coating is frequently used to create patterned polymer surfaces [13-15]. Similarly, in the development of optical devices, spin coating is used to create thin polymer blended films for anti-reflective coatings [13, 16-18]. In the textile industry, polymer blends are used to form fibers with desired properties [19-20]. Blended polymers are also used as protective coatings [21]. In all these applications, the immiscibility of polymers, solvent diffusion, interaction energies between the surfaces, wettability, etc., influence the final surface concentrations and morphologies of the polymer systems [15, 22-24]. As a result, the surface concentration of these mixed systems do not represent the bulk concentrations utilized. For example, in the case of spin-coating, the surface concentration of the thin

films would not be equivalent to the bulk concentration of the spin-coated emulsions [15, 22-24]. Frequently used methods to measure this surface concentration are often complicated and costly such as the X-ray photoelectron spectroscopy, Fourier transform infrared spectra, or atomic force microscopy [15, 22-24].

In addition to the need to understand and properly measure the surface adhesion, and its dependence on the surface concentration of blended polymer films, the characterization of the surface morphology and homogeneity is crucial. Different properties such as optical reflectance and light transmission, as well as the adhesive strength would be severely influenced by the morphology and uniformity of the blended films. Thus, a means of quantifying such a uniformity becomes imperative. Various approaches are used to characterize the spatial uniformity in the ecological, geological, textile, nano-materials, etc. contexts [25-29].

The present work aims at measuring the adhesive energy between the blended polymer film and a monolithic polymer film consisting of one of the components. To facilitate characterization of the adhesive energy, a novel, efficient and straightforward method of characterization of the surface topography of blended polymer systems is introduced. This method employs selective staining of individual polymers at the surface.

2. Experimental Methods

2.1 Materials

Two commercially available polymers were chosen for this work, PCL (M_n= 80 kDa) and N6 (molecular weight of each polymer repeat unit 104.83 Da [30]). The glass

transition temperatures of PCL and N6 are -64 °C [31] and 62.5 °C, respectively, whereas their melting temperatures are 60 °C and 228.5 °C, respectively. The polymers were used as received without any further purification. Where not specified, properties were obtained from the manufacturer. The solvents that were used here were acetic acid (grade 99≥%) and formic acid (grade ≥95%). For the surface characterization and selective staining, Rhodamine B (basic violet 10) dye was utilized. All the materials were obtained from Sigma Aldrich.

2.2 Sample Preparation

Sample preparation is depicted in Fig. 1. Spin coating was conducted as follows. Thin, rectangular copper wafer platelets of dimensions 60 mm × 30 mm with a 3 mm hole at the center were used as the base for spin coating. Note that the copper wafers were polished with a 1000 grit sandpaper. After the copper wafers were polished, they were rinsed thoroughly with ethanol and exposed to open air for one day. This allowed them to develop an inert copper oxide layer on the surface which would minimize reactions between the copper surfaces and the solvents used during the following spin-coating process. The center hole in these wafers aimed the subsequent blister test where adhesion energy is to be measured. One opening of the hole in the copper wafers was covered with a tape prior to the wafer being placed into the spin-coating setup, taped side down, as shown in Fig. 1a.

Either a 0.5 mL drop of the 15 wt% PCL solution or a drop of an emulsion of PCL in N6 was placed at the center of a copper wafer on the spin-coater. The 15 wt%

PCL solution used was prepared by dissolving PCL in a 1:1 ratio (by weight) mixture of the acetic acid and formic acid. Similarly, three separate emulsions of PCL in N6 were prepared for spin coating. The first emulsion contained 70 wt% PCL and 30 wt% N6; the second emulsion contained 60 wt% PCL and 40 wt% N6; and the third emulsion contained 40 wt% PCL in 60 wt% N6. These emulsions were prepared by mixing the 15 wt% PCL solution with a 20 wt% N6 solution prepared in the same 1:1 ratio (by weight) mixture of the acetic and formic acid. After thoroughly mixing, the polymer solutions were left for 30 min before spin-coating, permitting spinodal decomposition of the co-dissolved polymers and formation of clearly visible droplets of PCL in N6 matrix, or N6 in PCL matrix, i.e. the emulsion formation similarly to [32].

After depositing a 0.5 mL droplet on the copper wafers on the spin-coater, they were spun at 2700 rpm to form thin films from 70 % PCL spin-coated substrates using the 70 wt% PCL to 30 wt% N6 emulsion, or 60 % PCL spin-coated substrates using the 60 wt% PCL to 40 wt% N6 emulsion, or 40 % PCL spin-coated substrates using the 40 wt% PCL to 60 wt% N6 emulsion. In addition, monolithic thin films on copper wafers were spin-coated from the 15 wt% of PCL. It should be emphasized that after spin-coating, the pre-drilled holes in the copper wafers were not filled with polymer solutions or emulsions despite being exposed to the solution during spin-coating. The samples were then left for two days for the solvents to fully evaporate. The process resulted in the approximately 0.1 mm thick blended (PCL with N6) films (substrates) adhering to the underlying copper wafers (cf. Fig 1b).

The samples thus prepared were characterized using two methods. First, images of the resultant surface topography of the blended polymer substrates were obtained using

the novel staining method. Namely, N6 at the surface of the blended polymer films was selectively stained. Images were then obtained of these selectively stained films, and through an image analysis described in detail in subsection 2.5, the surface topography was evaluated. These polymer films were also used in the blister tests to measure the adhesion energy, as described in detail in subsection 2.4.

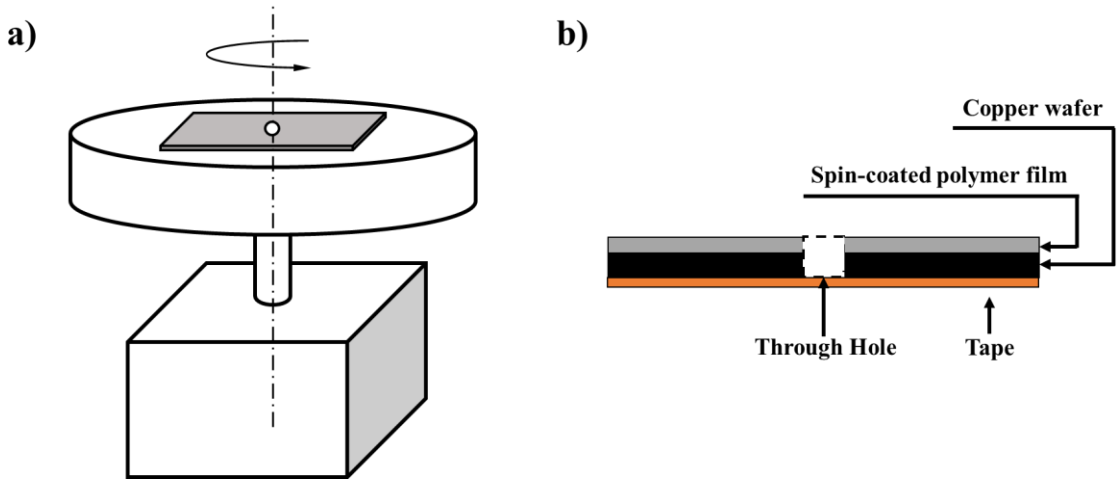

Figure 1. (a) Schematic of the spin-coating setup with copper wafer placed on top. (b) Cross-sectional view of the spin-coated polymer film composed of either monolithic PCL or blended PCL and N6 spin-coated on the copper wafer.

The monolithic PCL films used to measure adhesion energy were formed by spin coating. An aluminum petri dish (53 mm in diameter) was uniformly coated by 2 mL of the 15 wt% PCL solution. The PCL solutions in such petri dishes were left on a hotplate at 45 ± 2 °C to facilitate evaporation and formation of the PCL films. The films were left for two days for the solvent to fully evaporate. After that, these monolithic PCL films

were removed from the petri dishes and located onto the spin-coated substrates, forming a sandwich that was heat-treated at 55 ± 2 °C, below the glass transition temperature of N6, 62.5 °C. As described in the following subsection 2.3, adhesion would not occur between PCL and N6 at this temperature. The spin-coated blended substrates which were thermally adhered to the monolithic PCL films consisted of 100 % PCL, 70 % PCL, 60 % PCL, and 40 % PCL (with the rest being N6).

To further observe the effect of heat treatment on the adhesion between PCL and N6 and to characterize the surface structure by the selective staining with Rhodamine B, additional thin PCL films and N6 films were formed. These monolithic thin films were formed by spinning pure PCL or pure N6 solutions on the spin-coating setup shown in Fig. 1. In this case, a sheet of aluminum foil acting as the substrate was placed onto the spin-coating setup (instead of the copper platelet), and a 1.5 mL of the 15 wt% PCL solution was used to form monolithic PCL films. Alternatively, a 20 wt% N6 solution was used to form monolithic N6 films. In both cases the solvent was a 1:1 ratio (by weight) of acetic acid and formic acid. These solutions were spun for 30 s at 170 rpm. The aluminum foil with the thin film of polymer solution was then removed from the spin coater and placed onto a hotplate for 2 days to facilitate evaporation. In the case of PCL, the hotplate was set at the temperature of 45 ± 2 °C, while in the case of N6, it was set at the temperature of 60 ± 2 °C. It should be emphasized that formation of N6 films by a simple evaporation method in an aluminum petri dish is not robust and yields non-uniform films. After these monolithic PCL and N6 films were solidified, they were removed from the hotplates and used to evaluate their adhesion energy to one another at

temperatures below the glass transition of N6. These films were also used in the staining experiments described in subsection 2.5.

2.3 Sample Heat-Treatment

The spin-coated substrates containing either monolithic PCL or the PCL and N6 blends were placed (with the attached copper wafer down), onto a hotplate at 55 ± 2 °C. Then, the monolithic PCL films were placed onto the polymer side of the substrates, and a copper block pre-heated to the same temperature as the hotplate was placed onto these films, applying a low constant pressure of 0.01 MPa to facilitate an initial adhesion. The samples were heated for 180 s in this sandwich-like configuration, shown in Fig. 2.

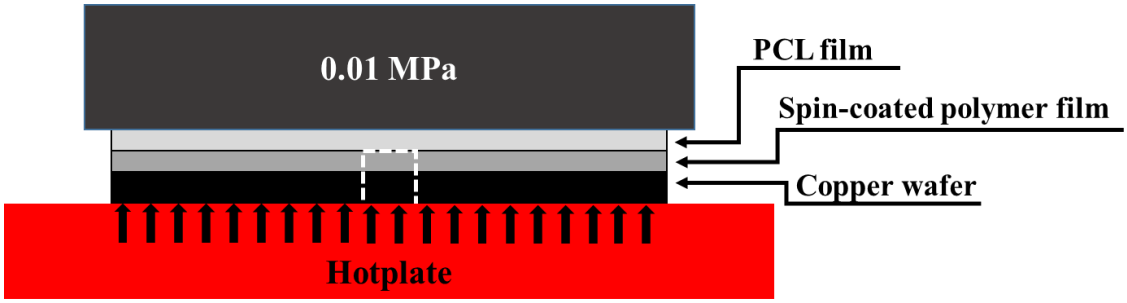

Figure 2. Schematic depicting conduction heating process used to heat-treat and adhere monolithic PCL films to different spin-coated substrates. The same approach was used in the attempt to thermally adhere the monolithic PCL films to the monolithic N6 films.

After the 180 s heat treatment, the pre-heated copper block was removed, and a steel roller of radius 30 mm was pressed to the substrates and rolled manually to remove air bubbles and facilitate uniform conglutination in the still hot samples. This was

conducted 20 consecutive times similar to [33]. The corresponding pressure applied by the roller can be found using the following equation [33-34]

$$L = \left[\frac{3(1-\nu^2)RF}{4E} \right]^{1/3} \quad (1)$$

where L is the half-width of the roller contact area, E is the Young's modulus of the steel roller, ν is the Poisson's ratio of the steel roller, R is the radius of the roller, and F is the force applied by hand-pressing.

The pressing force measured by a balance was F ≈ 9.8 N. The material properties of the steel roller are E = 200 GPa and ν=0.3. The radius of the roller was R = 44.62 mm. Then Eq. (1) yields the half-width L as 114 μm. Thus, the applied pressure which can be calculated as $p = F/(2L \times W)$, with the width W = 30 mm, was p=1.8 MPa. This shows that a sufficient load was applied to laminate the samples and remove the entrapped air-bubbles. Furthermore, this pressure also facilitated adhesion between the monolithic PCL film and the underlying blended polymer substrates. After heating and lamination, the samples were cooled to room temperature and used in the blister tests detailed in the following subsection 2.4.

It should be emphasized that the temperature of heat-treatment, 55 °C, is below the glass transition temperature of N6 and thus, the monolithic N6 films should not adhere to the monolithic PCL films [1, 5, 35-39], which was confirmed by the present results.

2.4 Blister Tests of Heat-Treated Samples

Blister tests are widely used to measure the adhesion energy between two materials [33, 40-43]. The blister-test setup, shown in Fig. 3, was built to measure the adhesion energy of the heat-treated samples. The heat-treated substrates were fixed in position. Then, a 0.5 mm diameter needle was advanced by a micrometer stage through the through-hole in the copper wafer to apply a force and delaminate the overlying spin-coated monolithic PCL film adhered to the underlying polymer substrate. The resistive force experienced by the 0.5 mm needle due to the delamination of the PCL film from the underlying polymer surface was measured by a force gauge (Inda model DS2-11). It should be emphasized that the blended films were fixed on the copper substrates, and thus did not contribute to the adhesion energy values measured in the blister test. Note also that blister tests were conducted at a fixed lowest rate of strain of about 0.3 mm/min. At such a low rate of strain mechanical behavior of PCL films, and thus the measured adhesion energy is unaffected by the strain rate (which is corroborated by stretching of PCL films using Instron machine). A DSLR camera, along with light sources, was used to obtain video recordings of the blister profile during the entire process. These recordings were then interpreted in conjunction with the load measured by the force gauge to obtain the adhesion energy.

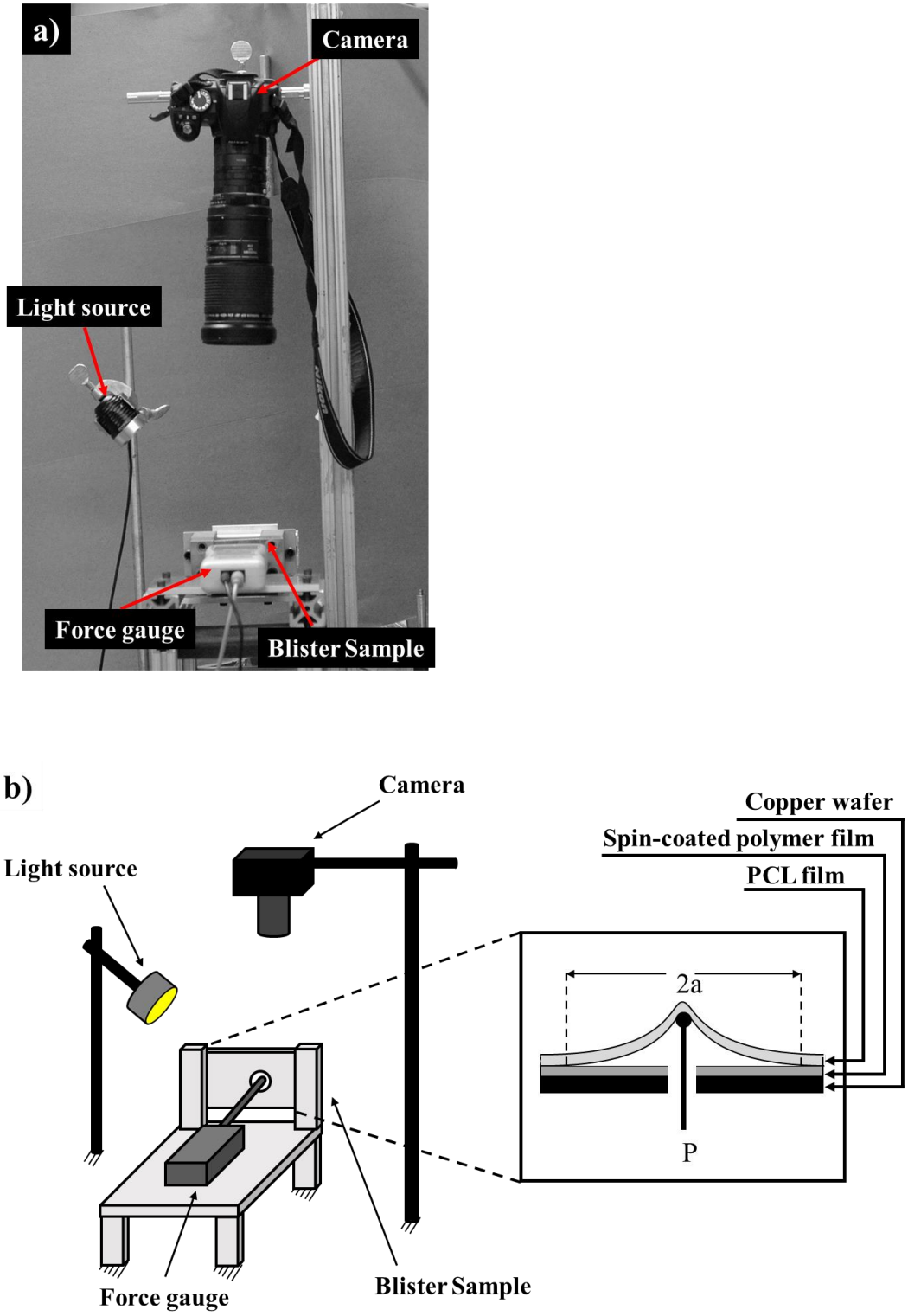

Figure 3. (a) Image of the blister test setup. (b) Schematic depicting the blister test setup with the observation system used to measure the blister profile. Here the maximum force

P measured before the complete delamination or failure of the sample, as well as the maximum blister diameter 2a are shown.

Using the blister profiles obtained from the images and the corresponding applied loads, the adhesion energy between the PCL film and different spin-coated polymer substrates was found using the following equation [33]

$$T = \frac{3}{8}\left(\frac{P^4}{\pi^4 E h a^4}\right)^{1/3} \quad (2)$$

where T is the adhesion energy, P is the maximum load measured before blister failure, E is the Young's modulus of the PCL layer, h is the thickness of the PCL layer, and a is the measured blister radius.

2.5 Selective Staining

During the spin-coating process, the surface concentration of a polymer in a blend would not necessarily be equivalent to that of the emulsion used during spin-coating [15, 22-24]. To characterize the surface composition and uniformity in spin-coated substrates, a novel method of selective staining is used in the present work. It stems from the ability of the Rhodamine B dye to selectively stain only N6 in the N6-PCL blends at the surface of the blended spin-coated films.

To reveal the ability of selective staining of N6, monolithic thin films of PCL or N6 were independently dipped into a Rhodamine B solution. The Rhodamine solution

used for dyeing was a 0.02 wt% solution of Rhodamine B dissolved in DI water. This solution was kept heated on a hotplate at 90 °C. Then, small rectangular pieces, approximately 3.5 cm × 8.0 cm, of either thin monolithic PCL films or monolithic N6 films were submerged for 10 s into the solution. After that, the films were removed and rinsed with DI water at room temperature. After the rinsing, additional DI water was poured over the films and subsequently patted dry with a clean towel. Several images of samples before and after dyeing are shown in Fig 4.

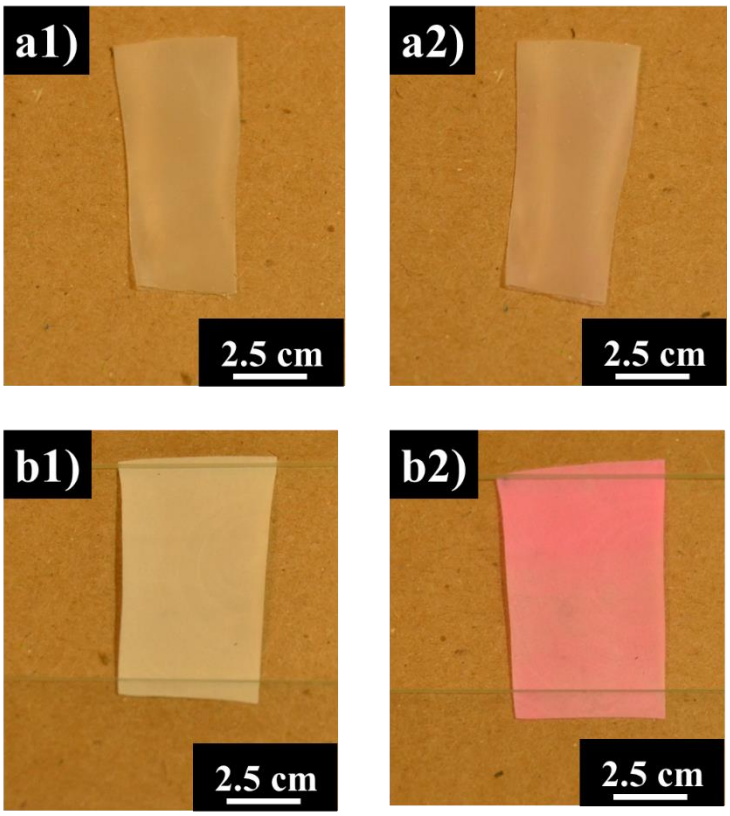

Figure 4. Sample images before and after submerging monolithic PCL and N6 films in the Rhodamine B solution. Panel (a1) depicts a PCL film submerging, and panel (a2) – after it has been submerged. Panel (b1) depicts a N6 film before submerging, and panel (b2) – after it has been submerged.

Figure 4 shows that Rhodamine B does not dye PCL, whereas it clearly dyes N6. According to [44], the anion of Rhodamine B dye attaches to the amide bond of N6 owing to the unbalanced charge, whereas in the case of PCL there is no such unbalanced charge. Thus, Rhodamine B dye does not attach to PCL. This makes selective staining of a single component at the surface of PCL-N6 blended polymer substrates possible.

The spin-coated samples of 70 % PCL, 60 % PCL, and 40 % PCL were selectively stained. After that, surface images of such samples were obtained by using LED illumination. The images of a total area of 2.03 cm^2 were then taken by a DSLR camera (cf. Fig. 5a). The aperture settings on the camera was f = 7.1 and the exposition time was 1/5.

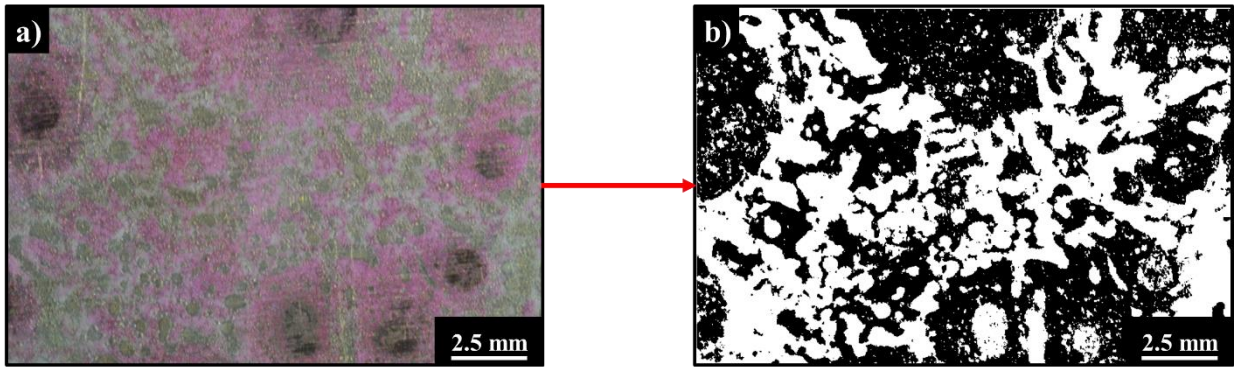

Figure 5. Images of a dyed spin-coated blended PCL-N6 sample before and after processing. Panel (a) depicts the original image, and panel (b) depicts the processed image converted to black and white, with white corresponding to PCL and black corresponding to N6.

The images of stained blended samples were then analyzed using an in-house image analysis code developed on the Matlab R2016 platform. The original color images were converted to black and white binary images in such a way that white corresponded to the PCL domains, and black – to the dyed N6 domains (cf. Figs. 5a and 5b). The threshold value for converting color images to black and white images was kept same for all the images. Five images from distinct locations on two samples of each of the blended polymer spin-coated substrates (70 % PCL, 60 % PCL, and 40 % PCL) were analyzed using this image analysis software. Using these binary images, information on the resultant PCL surface concentration, as well as the uniformity of the spin-coated films can be readily evaluated, as described in detail in subsection 2.6.

2.6 Surface Topography Analysis

To calculate the surface concentrations, a Matlab code was developed in which each binary image of the various spin-coated substrates was converted into a two-dimensional binary array. Namely, each pixel of the binary image was assigned a value of "0" corresponding to white (i.e. PCL), or "1" corresponding to black (i.e. N6). Using this binary array, the total area fraction of white can be calculated. This corresponds to the surface concentration of PCL in the various blended polymer substrates.

Sample homogeneity and uniformity can be assessed using the stained blended substrates. Various approaches were used in different fields for this purpose [25-29]. The most widely used approach is based on the quadrant method, which employs such statistical characteristics as the index of dispersion [26]. Another statistical characteristic,

the uniformity index, was used in the textile-oriented applications [28]. In the present work, both statistical characteristics were evaluated. Note, that according to [26] the index of dispersion is expected to be the most robust and reliable.

The uniformity was characterized as follows. The resultant binary (black and white) two-dimensional array is expressed as a matrix of pixels. It is subdivided into n rectangles, with $n = i^2$, with i being an integer greater than 1 (cf. Fig. 6).

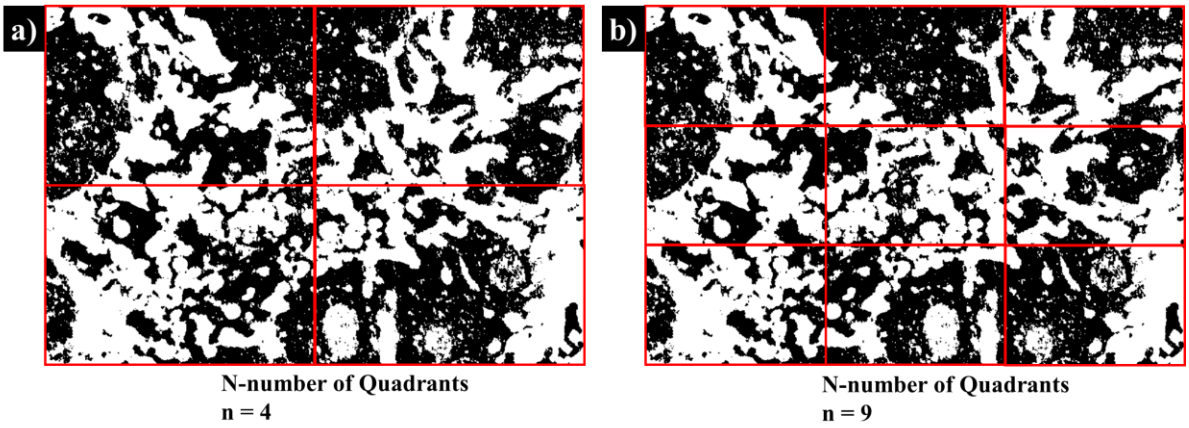

Figure 6. Subdivision of a processed image into n rectangles. Panel (a) depicts the case of n = 4 , and panel (b) – of n = 9 equally-sized rectangles.

For each rectangle, the white fraction (PCL) f_o is measured. The index of dispersion, I, is found as

$$I = \frac{\sigma^2}{\bar{x}} \qquad (3)$$

where σ^2 is the observed variance and $\bar{x}$ is the observed mean of the white faction f_o measured for different rectangles. Note that the value of I uniformity depends on the

number of rectangles n used. The value of n was chosen so that the value of I would change only slightly with n.

The index of dispersion as a function of the number of divisions of the binary images depicted in Fig. 5 is shown in Fig. 7. It is seen that saturation is reached at about n=50 and the plateau value $I \approx 0.75$.

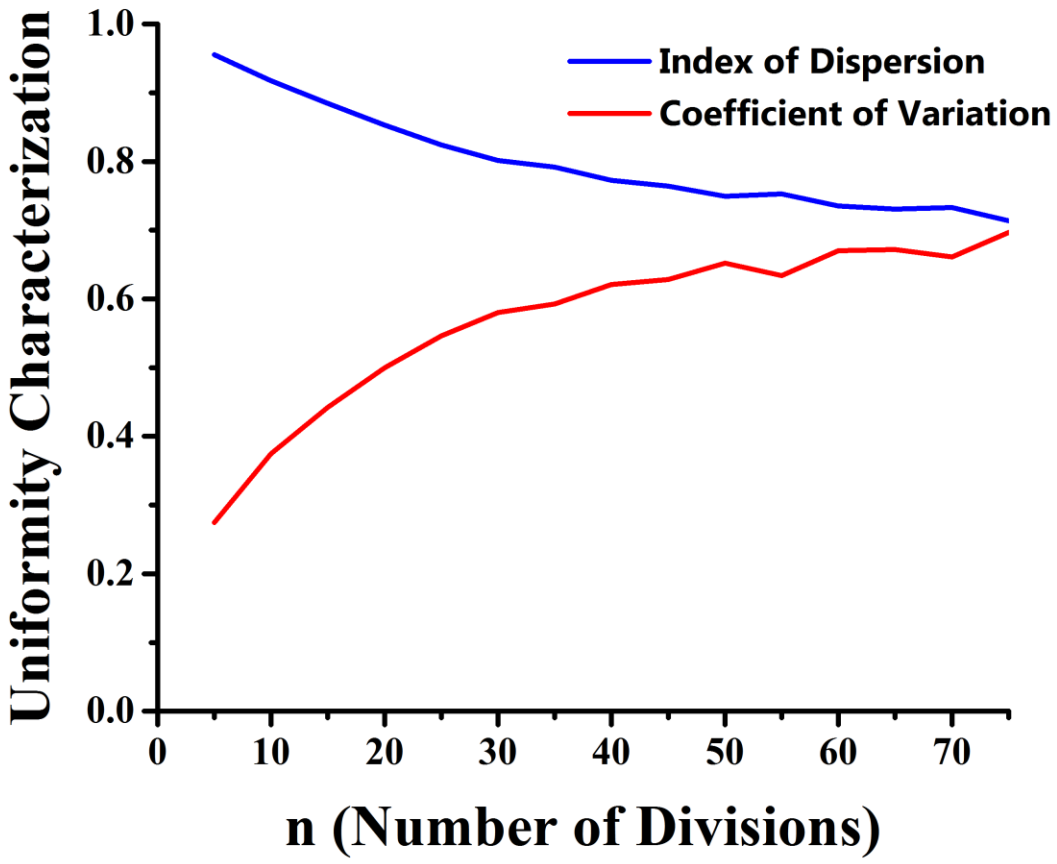

Figure 7. The index of dispersion (blue) and the coefficient of variation (red) with the number of divisions n.

The coefficient of variation, CV, is defined as

$$CV = \frac{\sigma}{\bar{x}} \tag{4}$$

It also depends on the number of divisions n and saturates at about n=50 to 60 at the value of $CV \approx 0.65$ (cf. Fig. 7). This means that at n=50 to 60, the value of σ=I/CV=1.15. Using the results of Fig. 7, in the present work the images were divided into 50 rectangles.

It should be emphasized that for each number of rectangles n, the chi-squared value χ_n^2 , which represents the goodness-of-the-fit, can be measured as [25, 28-29].

$$\chi^2{}_n = \sum \frac{(f_e - f_o)^2}{f_e} \tag{5}$$

where f_e is the expected white fraction, and f_o the observed white fraction for each subdivision number. The index describing the resultant χ^2 distribution, the uniformity index UI is then obtained as [25, 28].

$$UI = \left(1 - \frac{\sum_{i=2}^{i=i_{max}} \chi^2{}_i}{\sum_{i=2}^{i=i_{max}} (n_i - 1)} \right) \times 100\% \tag{6}$$

The uniformity index UI varies between 0% and 100%, with 100% corresponding to the case of perfect uniformity. Note that i_{max} is the maximum number of rectangles into which the binary image was divided. The upper bound of the summation, i_{max}, in Eq. (6) is limited as the n-number of divisions reaches the size of a pixel. However, well before reaching the size of a pixel, the resultant uniformity index would cease to significantly alter and plateau to a constant value. Thus, a total number of rectangles n for the

calculation of UI was used at this plateauing limit. A Matlab code was developed to measure UI according to Eq. (6). The predicted values of UI found from the images of Fig. 5 are shown in Fig. 8.

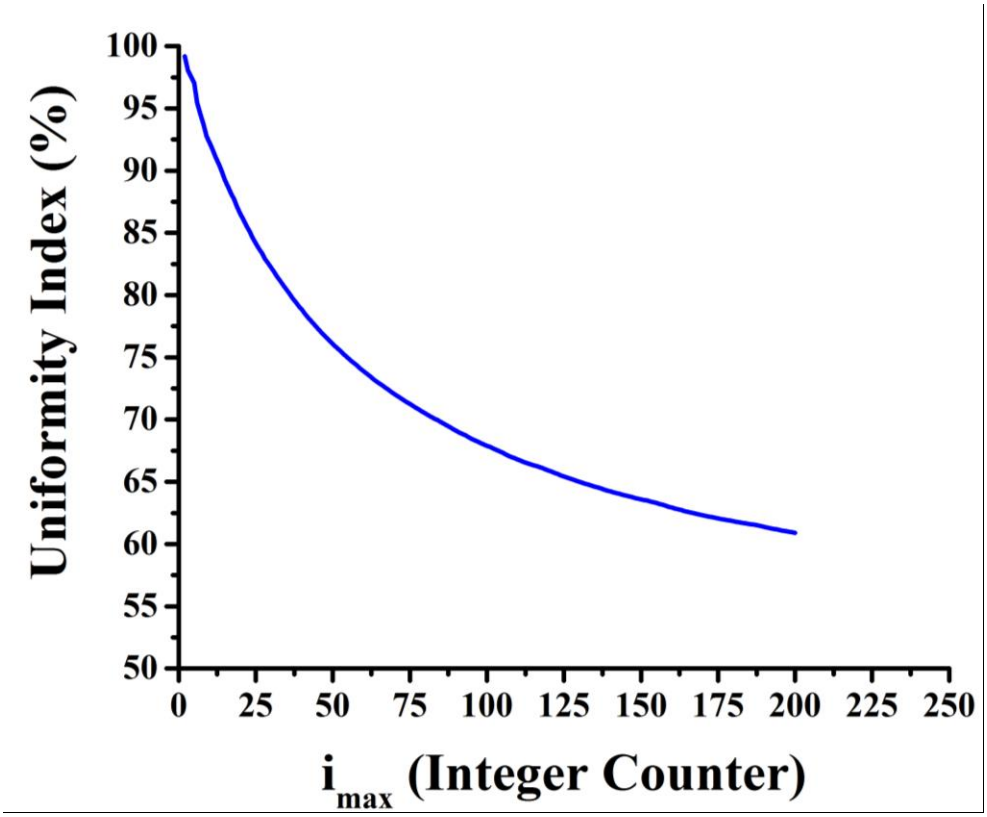

Figure 8. Uniformity index calculated for the binary image shown in Fig. 5 using Eq. (6) for various number of rectangles n. Note that $n = i^2$, where n is the maximum number of rectangles in the image.

Figure 8 shows that as the number of divisions into rectangles surpasses 150, the UI value saturates at about $U \approx 60\%$. Accordingly, $i_{max} = 150$ was chosen in this work.

3. Results and Discussion

3.1 Blister Tests of Heat-treated Samples

Blister tests were conducted with the monolithic PCL films thermally adhered at 55 °C to the 100 % PCL spin-coated substrates, as well as with the blended 70 % PCL, 60 % PCL, and 40 % PCL spin-coated substrates. Multiple blister tests for each of these cases were conducted. Namely, in the case of the monolithic PCL spin-coated substrates, 11 trials were conducted, whereas in the case of the blended 70 wt% PCL, 60 wt% PCL, and 40 wt% PCL, 6, 15, and 9 trials were conducted, respectively. The results for the average adhesion energy found using Eq. (2) for all the cases of spin-coated substrates are listed in Table 1. The Young's modulus of PCL according to [45] is E=343.9-364.3 MPa, thus the value of E=354.1 MPa was used. The measured adhesion energies for all the tested spin-coated substrates were also normalized by the average adhesion energy for the case of monolithic PCL spin-coated substrates. The results for this normalized average adhesion energy for all the cases of the spin-coated substrates are shown in Fig. 9. Several examples of the recorded blister profiles for all the cases of the spin-coated substrates are shown in Fig. 10.

Spin-coated substrate	**Adhesion energy (J/m^2)**
100 % PCL	7.91 ± 2.98
70 % PCL	7.41 ± 0.67
60 % PCL	6.81 ± 2.22
40 % PCL	4.24 ± 1.26

Table 1. Average adhesion energy for all the tested heat-treated samples.

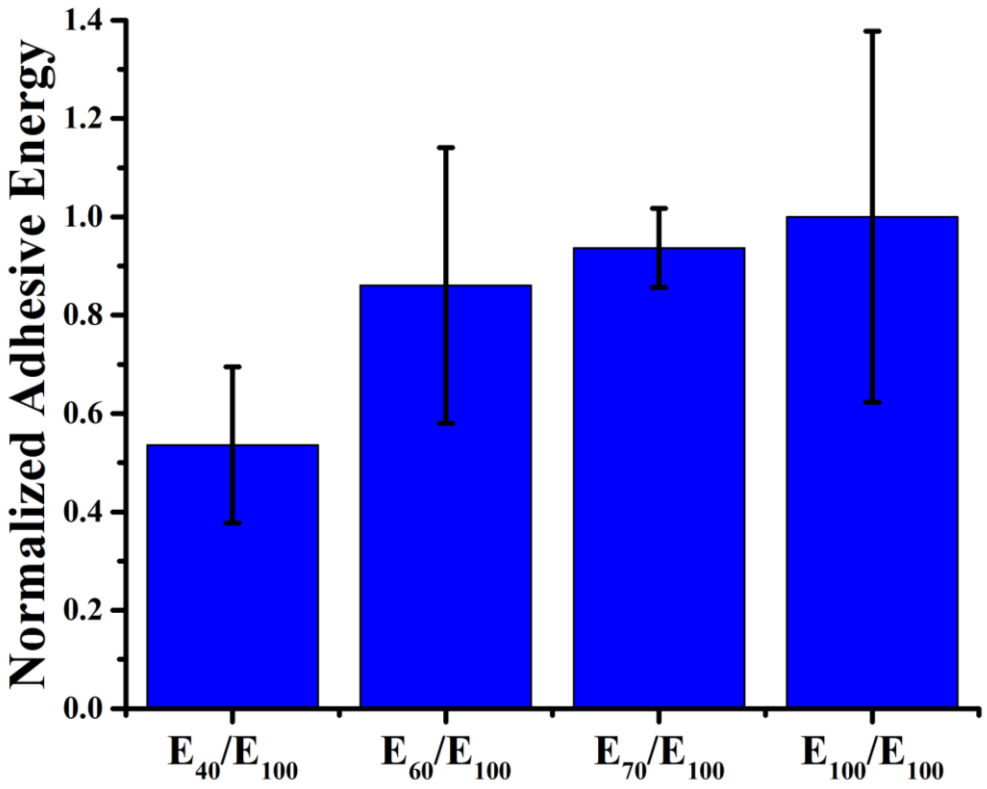

Figure 9. Normalized adhesion energy of the heat-treated samples. E_{100}/E_{100} corresponds to the case of 100 % PCL in the substrate (monolithic PCL film adhered to PCL), E_{70}/E_{100} corresponds to the normalized adhesion energy for the case of 70 % PCL in the substrate adhered to PCL. E_{60}/E_{100} corresponds to the case of 60 % PCL in the substrate adhered to PCL, and E_{40}/E_{100} - to the case of 40 % PCL in the substrate adhered to PCL. The error bars in these normalized results reflect the standard deviation in the results listed in Table 1.

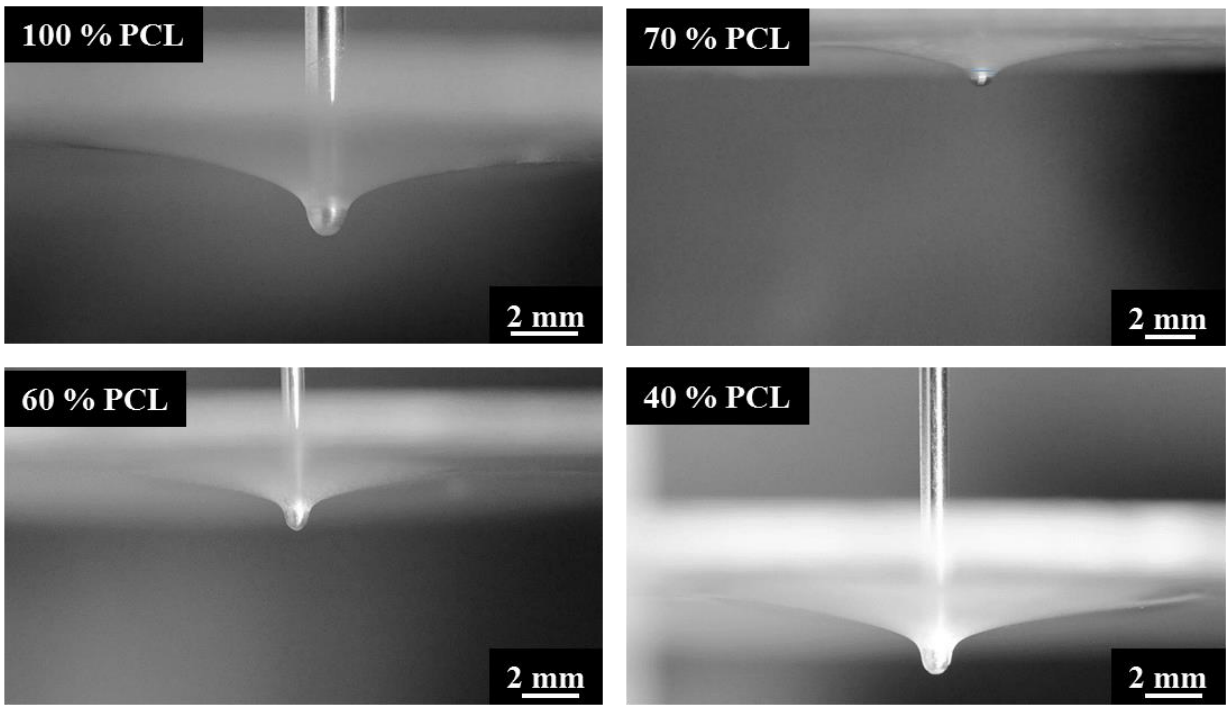

Figure 10. Blister profiles for different heat-treated samples.

Also, it was observed that PCL does not thermally adhere onto N6 at the chosen temperature of 55 °C. This is due to the fact that the glass transition temperature of N6 was not achieved, which is a known requirement for the adhesion between polymers [1, 5, 35-39]. Thus, the normalized adhesive energy shown in Fig. 9 should be associated with the surface concentration of PCL, since the adhesion only occurred between the monolithic PCL films and the PCL islands at the surface of the spin-coated blended substrates. An additional possibility of the presence of PCL-N6 mixed domains and their effect on the adhesion energy is discussed in sub-section 3.3.

3.2 Surface Topography Measurement

Surface mapping of PCL on the spin-coated blended substrates of 70 % PCL, 60 % PCL, and 40 % PCL was conducted using the method of selective staining. After dyeing, five images from distinct locations on the two samples of each stained spin-coated substrates, namely the 100 % PCL, 70 % PCL, 60 % PCL, and 40 % PCL, were processed and converted into binary images. Here, two images were taken at opposite sides of the through hole, along the length of 60 mm, for each sample, resulting in four images or locations, while the fifth image was additionally taken toward the edge of one of these samples. The results for all the locations on spin-coated substrates, as well as the average and standard deviation are listed in Table 2. Several characteristic images of the selectively stained blended samples of 70 % PCL, 60 % PCL and 40 % PCL, as well as the processed binary images are shown in Fig. 11. Note, N6 islands at the surface of the substrates was dyed pink, leaving only PCL undyed.

Table 2 reveals that the average surface concentrations of PCL are somewhat different from the volume fraction of PCL in the film. In fact, the surface concentration varies widely between different locations. This can be attributed to the fact that both polymers have different macromolecular structure, chain length, polymer-solvent interaction, polymer-polymer miscibility, diffusion coefficient in solvent, the interaction energies, etc. [15, 22-24, 46]. This results in an uneven localization of PCL and N6 over the surface of the blended samples.

It should be emphasized that on averaging the surface concentration of PCL, the results did not reveal a wide variation across the samples.

Percent surface concentration of PCL

	70 % PCL	60 % PCL	40 % PCL
Location 1	85 %	56 %	51 %
Location 2	65 %	63 %	50 %
Location 3	70 %	51 %	53 %
Location 4	72 %	62 %	35 %
Location 5	62 %	61 %	43 %
Average	71 ± 9 %	59 ± 5 %	46 ± 7 %

Table 2. Surface concentration of PCL for all observed locations of the two samples of the spin-coated blended substrates containing 70 % PCL, 60 % PCL, and 40 % PCL.

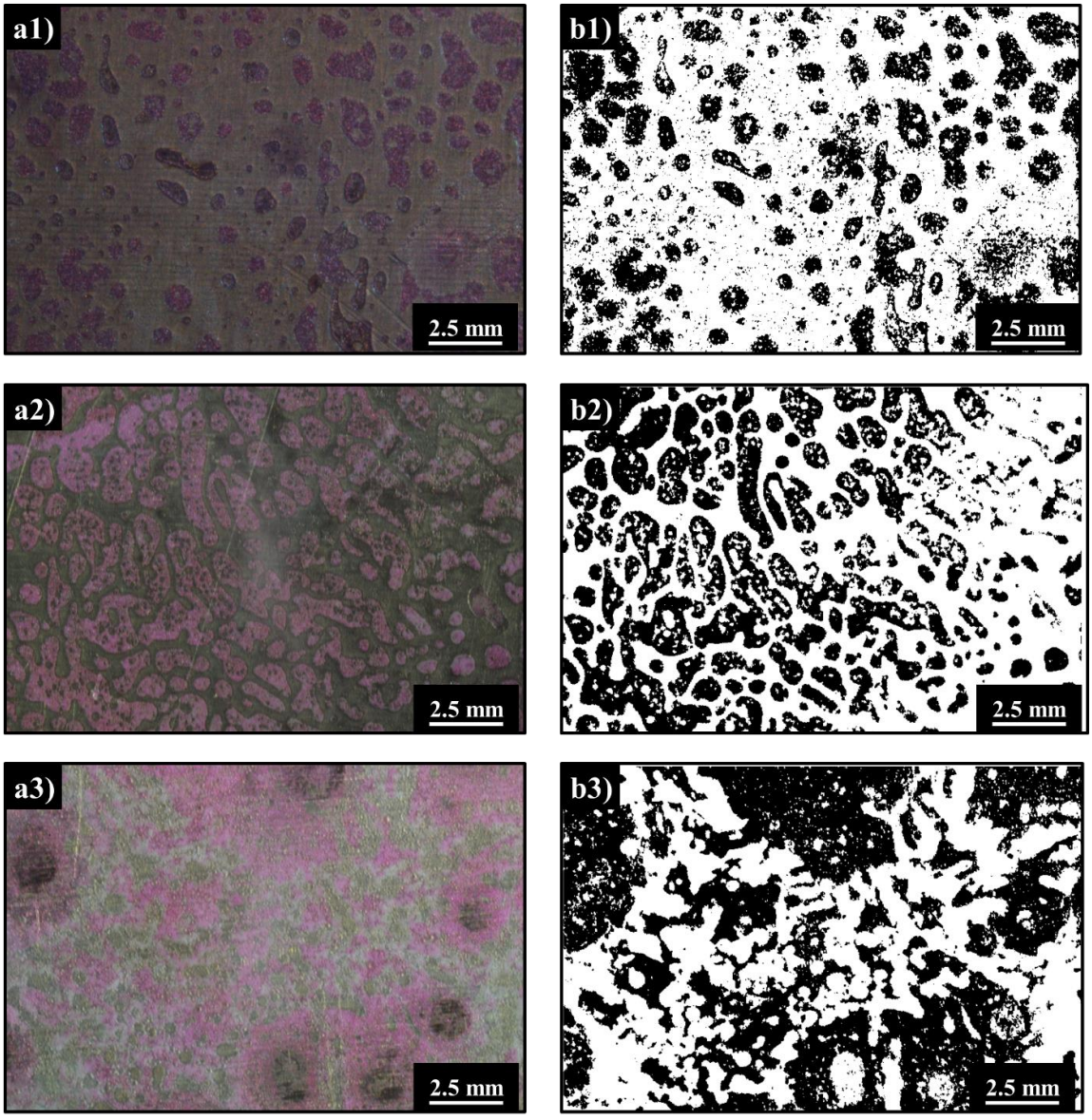

Figure 11. Images of the selectively stained spin-coated blended samples before and after processing. Panel (a1) depicts the dyed spin-coated film of 70 wt% PCL, and panel (b1) depicts the processed binary black and white image, with white corresponding to PCL and black corresponding to N6. Panel (a2) depicts the dyed spin-coated film of 60 wt% PCL, and panel (b2) depicts the processed binary black and white image. Panel (a3) depicts the dyed spin-coated film of 40 wt% PCL, and panel (b3) depicts the processed binary black and white image.

The statistical characteristics of the surfaces of the blended samples obtained from the binary images of Fig. 11 are shown in Table 3. The data for the uniformity index are listed in Table 4.

Index of Dispersion / Coefficient of Variation			
	70 % PCL	**60 % PCL**	**40 % PCL**
Location 1	0.82 / 0.53	0.77 / 0.61	0.75 / 0.65
Location 2	0.83 / 0.48	0.84 / 0.49	0.69 / 0.80
Location 3	0.75 / 0.65	0.68 / 0.80	0.77 / 0.62
Location 4	0.87 / 0.43	0.83 / 0.49	0.64 / 1.01
Location 5	0.86 / 0.43	0.78 / 0.65	0.74 / 0.95
Average	0.83 / 0.50	0.78 / 0.61	0.72 / 0.81

Table 3. The index of dispersion and coefficient of variation of PCL at the surfaces of the spin-coated blended 70 % PCL, 60 % PCL, and 40 % PCL substrates.

Uniformity Index of PCL			
	70 % PCL	**60 % PCL**	**40 % PCL**
Location 1	77 %	69 %	64 %
Location 2	83 %	76 %	64 %
Location 3	75 %	65 %	66 %
Location 4	83 %	75 %	59 %
Location 5	83 %	74 %	70 %
Average	80 ± 4 %	72 ± 5 %	65 ± 4 %

Table 4. The uniformity index of PCL at the surface for all observed locations of the two separate samples of each of the spin-coated blended substrates containing 70 % PCL, 60 % PCL, and 40 % PCL.

The statistical characteristics listed in Tables 2-4 show that as the PCL concentration increased, the uniformity of PCL distribution over the sample surface increased as well. This has a direct impact on the adhesion energy of the blended samples with the monolithic PCL film described next.

3.3 Blister Test Results versus Surface Topography

The results of the blister tests for the adhesion energy listed in Table 1 and depicted in Fig. 9 elucidate the polymer-polymer adhesion (or its absence) between PCL and N6. A decrease in the PCL concentration at the surface of the spin-coated blended substrates reduced the adhesive energy to the overlying monolithic PCL film, since PCL had not adhered to N6 at the surface. The measured normalized adhesive energies shown in Fig. 6 are, to some extent, linked to the surface concentration of PCL in the spin-coated blended films. However, the measured values of the normalized adhesion energy E_i/E_{100}, with i=40, 60, 70 and 100 are not linearly proportional to the measured surface concentrations of PCL of 71±9 %, 59±5 %, and 46±7 %, as Fig. 12 shows.

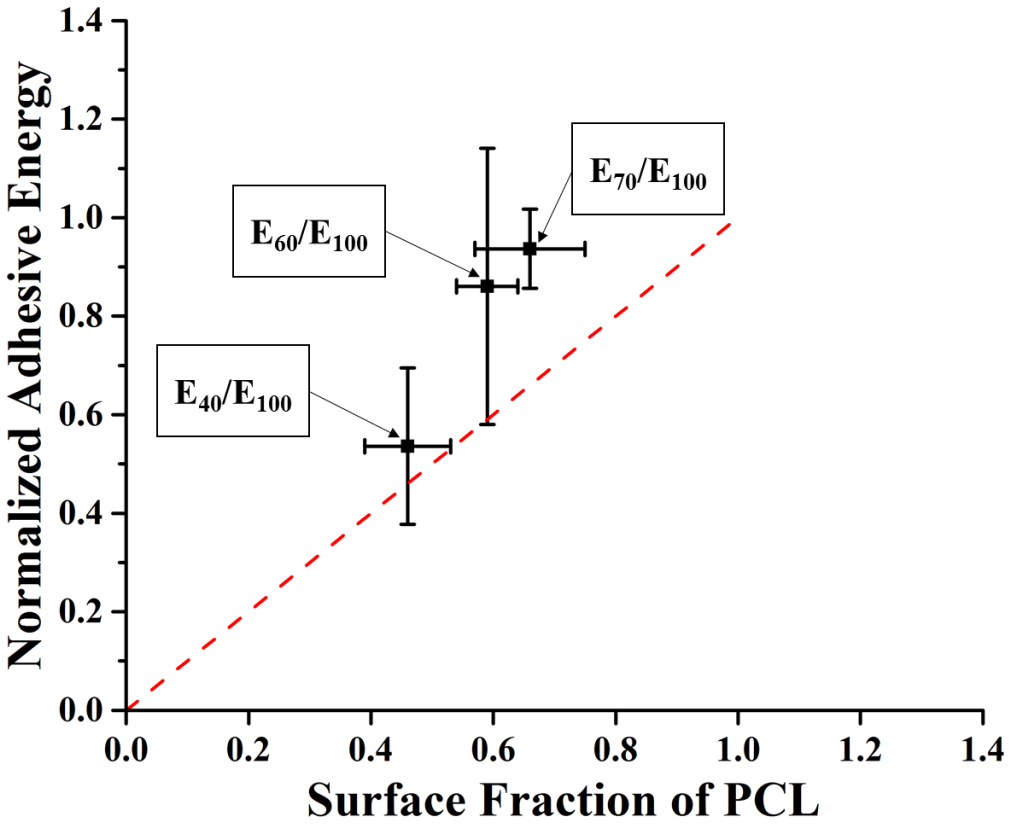

Figure 12. The normalized adhesion energy of the heat-treated blended samples versus the surface concentration of PCL. The vertical error bars correspond to the standard deviation of the results listed in Table 1, whereas the horizontal error bars correspond to the standard deviation of the results listed in Table 2. The dashed red line is inclined by 45°.

In the present work, the weight percentage of PCL in blend with N6 is significantly higher than the miscibility limit [47,48]. According to [47], full miscibility of PCL with nylon 6 is achieved at ~14-16 wt% PCL content. The ester groups of PCL

are oriented in the direction opposite to the main chain direction and conform to a N6 - like structure [48]. As a result, PCL can be mixed at low contents with nylon 6 and form a mutually entangled structure. It should be emphasized that in spite of the immiscibility of PCL and N6, their blend results in a durable film [48]. The tendency to the immiscibility associated with the ester-amide interactions [47], was attributed to a significant difference in the glass transition temperatures T_g of both polymers. At higher than ~14-16 wt% PCL content, a part of PCL stays unmixed (cf. Figs. 5 and 6, where digital photographs reveal the partial mixing of PCL, as well as the unmixed domains). This partition of PCL into mixed and unmixed parts explains the deviation from linearity in the dependence of the adhesive energy on the PCL content seen in Figure 12, ascertaining the fact that the still-mixed domains can also contribute to adhesion.

For the 70% blended sample the adhesion energy approached that of the monolithic PCL film (cf. Fig. 12). It should be emphasized that the present results have far-reaching implications for the industrial applications where polymer composites are produced extensively by adhering polymer layers by thermal bonding accompanied by pressurization. Most of those applications tend to replace a part of the polymer content by another filler to minimize cost, supposedly without losing the adhesion energy. This work shows that by achieving a higher uniformity of the matrix polymer in the composite film, the adhesive energy can be tuned to match that of the monolithic polymer film.

Note also the possible sources of experimental error in the adhesion tests conducted. There may have been an experimental inaccuracy in measuring the adhesion energy, namely the method of obtaining blister radii using an image analysis where the camera may have been slightly tilted relative to the sample. Reproducibility of forming

the substrates was also an issue. During formation of various spin-coated substrates, the copper on the wafer surface, albeit being partially passivated by the oxide layer, would still react with the solvents (the formic and the acetic acid). In addition, variations in humidity have been observed to severely alter the evaporation rate of various spin-coated blended substrates and monolithic PCL films. Finally, the heat treatment process can introduce variability. The substrates were heated at 55 ± 2 ℃, which is close to the melting point of PCL, 60 °C. Upon reaching the melting point, a strong adhesion would occur between the monolithic PCL films and the PCL contained at the surface of the various spin-coated blended substrates due to spreading of molten PCL over the surface of the blended samples.

4. Conclusion

The adhesive energy of blended and monolithic PCL and PCL-N6 surfaces was measured by blister method and linked to the surface composition of the blended samples. It was shown that PCL does not adhere to N6 after heat-treatment at 55 ± 2 °C, while the monolithic PCL films adhered to the blended samples via the PCL at the surface. Furthermore, an effect of partially mixed PCL-N6 domains on the adhesion energy has been elucidated.

The surface concentration of PCL in the blended samples was also established using a novel staining method. It was shown that the surface concentration of PCL differs from its bulk content in the blend samples. The measurements also revealed that the normalized adhesion energy between the blended PCL-N6 samples and monolithic PCL

films is related to the surface concentration of PCL. Due to the minor partial mixing of PCL with N6 during spin-coating, the measured surface concentration of PCL would remain an underestimate. However, this method may prove to be a useful first estimate in the measurements of surface concentration of blended films. Several statistical characteristics of the surfaces of the blended samples were also used to characterize their uniformity/non-uniformity. It was shown that increasing the surface uniformity of the adhering component in the blended samples (PCL), one increases the adhesion energy. Moreover, at about 70% of PCL at the surface, the adhesion energy of blended samples to monolithic PCL films could reach the value characteristic of the adhesion between two monolithic PCL samples.

Acknowledgement

This work is supported by the Nonwovens Institute, grant No. 14-163.

5. References

[1] H. R. Brown, Adhesion between polymers. J. Res. and Develop. 38.4 (1994), 379-389.

[2] P. J. Cole, R. F. Cook, C. W. Macosko, Adhesion between immiscible polymers correlated with interfacial entanglements, Macromolecules, 36 (2003), 2808-2815.

[3] C. Creton, E. J. Kramer, C. Y. Hui, H. R. Brown, Failure mechanisms of polymer interfaces reinforced with block copolymers. Macromolecules, 25 (1992), 3075-3088.

[4] K. L. Foster, R. P. Wool, Strength of polystyrene-poly (methyl methacrylate) interfaces. Macromolecules, 24 (1991), 1397-1403.

[5] A. Baldan, Adhesion phenomena in bonded joints, International Journal of Adhesion & Adhesives, 38 (2012), 95-116.

[6] A. Islam, H. N. Hansen, M. Bondo, Experimental investigation of the factors influencing the polymer-polymer bond strength during two-component injection moulding, Int. J. Adv. Manuf. Technol. 50 (2010), 101-111.

[7] T. B. Juhl, D. Bach, R. G. Larson, J. deClaville Christiansen, E. A. Jensen, Predicting the laser weldability of dissimilar polymers. Polymer, 54 (2013), 3891-3897.

[8] P.G. De Gennes, Weak adhesive junctions, Journal de Physique, 50 (1989), 2551-2562.

[9] H. Ji, P. G. De Gennes, Adhesion via connector molecules: the many-stitch problem. Macromolecules, 26 (1993), 520-525.

[10] K. P. O'Connor, T. C. B. McLeish, Entangled dynamics of healing end-gradted chains at a solid/polymer interface, Faraday Discuss., 98 (1994), 67-78.

[11] K. P. O'Connor, T. C. B. McLeish, "Molecular velcor": dynamics of a constrained chain into an elastomer network, Macromolecules, 26 (1993), 7322-7325.

[12] E. Raphael, P. G. De Gennes, Rubber-rubber adhesion with connector molecules. J. Phys. Chem., 96 (1992), 4002-4007.

[13] M. Böltau, S. Walheim, J. Mlynek, G. Krausch, U. Steiner, Surface-induced structure formation of polymer blends on patterned substrates, Nature, 391 (1998), 877-879.

[14] K. Norrman, A. Ghanbari-Siahkali, N. B. Larsen, 6 Studies of spin-coated polymer films. Annu. Rep. Sect. C, 101 (2005), 174-201.

[15] S. Walheim, M. Böltau, J. Mlynek, G. Krausch, U. Steiner, Structure formation via polymer demixing in spin-cast films, Macromolecules, 30 (1997), 4995-5003.

[16] M. Ibn-Elhaj, M. Schadt, Optical polymer thin films with isotropic and anisotropic nano- corrugated surface topologies, Nature, 410 (2001), 796-799.

[17] J. J. M. Halls, C. A. Walsh, N. C. Greenham, E. A. Marseglia, R. H. Friend, S. C. Moratti, A. B. Holmes, Efficient photodiodes from interpenetrating polymer networks, Nature, 376 (1995), 498-500.

[18] S. Walheim, E. Schäffer, J. Mlynek, U. Steiner, Nanophase-separated polymer films as high-performance antireflection coatings, Science, 283 (1999), 520-522.

[19] M. Afshari, R. Kotek, M. H. Kish, H. N. Dast, B. S. Gupta, Effect of blend ratio on bulk properties and matrix–fibril morphology of polypropylene/nylon 6 polyblend fibers, Polymer, 43 (2002), 1331-1341.

[20] D. S. Varma, V. K. Dhar, Studies of nylon 6/PET polymer blends: Structure and some physical properties, Journal of applied polymer science, 33 (1987), 1103-1124.

[21] H. Ade, D. A. Winesett, A. P. Smith, S. Qu, S. Ge, J. Sokolov, M. Rafailovich, Phase segregation in polymer thin films: Elucidations by X-ray and scanning force microscopy, EPL, 45 (1999), 526-532.

[22] K. Artyushkova, B. Wall, J. Koenig, J. E. Fulghum, Direct correlation of x-ray photoelectron spectroscopy and Fourier transform infrared spectra and images from poly (vinyl chloride)/poly (methyl methacrylate) polymer blends. Journal of Vacuum Science & Technology A, 19 (2001), 2791-2799.

[23] X. Li, Y. Han, L. An, Surface morphology control of immiscible polymer-blend thin films. Polymer, 44 (2003), 8155-8165.

[24] L. Cui, Y. Ding, X. Li, Z. Wang, Y. Han, Solvent and polymer concentration effects on the surface morphology evolution of immiscible polystyrene/poly (methyl methacrylate) blends, Thin Solid Films, 515 (2006), 2038-2048.

[25] G. Agarwal, L. Koehl, A. Perwuelz, The influence of constructional properties of knitted fabrics on cationic softener pick up and deposition uniformity, Textile Res. J., 80 (2010), 1432-1441.

[26] K. M. Kam, L. Zeng, Q. Zhou, R. Tran, J. Yang, On assessing spatial uniformity of particle distributions in quality control of manufacturing processes, Journal of Manufacturing Systems, 32 (2013), 154-166.

[27] M. Morisita, Measuring of the dispersion of individuals and analysis of the distributional patterns. Mem. Fac. Sci. Kyushu Univ. Ser. E, 2 (1994), 5-235.

[28] B. Pourdeyhimi, L. Kohel, Area-based strategy for determining web uniformity, Textile Res. J., 72 (2002), 1065-1072.

[29] B. Pourdeyhimi, B. Xu, L. Wehrle, Evaluating carpet appearance loss: periodicity and tuft placement, Textile Res. J. 64 (1994), 21-32.

[30] S. Sinha-Ray, M. W. Lee, S. Sinha-Ray, A. Seongpil, B. Pourdeyhimi, S. S. Yoon, A. L. Yarin, Supersonic nanoblowing: a new ultra-stiff phase of nylon 6 in 20–50 nm confinement, J. Mater. Chem. C 1 (2013), 3491-3498.

[31] J. Brandrup, E.H. Immergut, Polymer Handbook, John Wiley & Sons, New York (1989).

[32] A. V. Bazilevsky, A. L. Yarin, C. M. Megaridis, Co-electrospinning of core-shell fibers using a single-nozzle technique. Langmuir, 23 (2007), 2311-2314.

[33] M. W. Lee, S. An, H. S. Jo, S. S. Yoon, A. L. Yarin, Self-healing nanofiber-reinforced polymer composites. 2. Delamination/debonding and adhesive and cohesive properties, ACS Applied Materials & Interfaces, 7 (2015), 19555-19561.

[34] B. V. Derjaguin, V. M. Muller, Y. P. Toporov, Effect of contact deformations on the adhesion of particles, J. Colloid Interface Sci., 53 (1975), 314-326.

[35] Y. M. Boiko, G. Guerin, V. A. Marikhin, R. E. Prud'homme, Healing of interfaces of amorphous and semi-crystalline poly(ethylene terephthalate) in the vicinity of the glass transition temperature, Polymer, 42 (2001), 8695-8702.

[36] Y. M. Boiko, J. Lyngaae-Jorgensen, Healing of interfaces of high and ultra-high-molecular-weight polystyrene below the bulk T_g, Polymer, 45 (2004), 8541-8549.

[37] G. Guerin, F. Mauger, R. E. Prud'homme, The adhesion of amorphous polystyrene surfaces below Tg, Polymer, 44 (2003), 7477-7484.

[38] K. Jud, H. H. Kausch, J. G. Williams, Fracture mechanics studies of crack healing and welding of polymers, Journal of Materials Science, 16 (1981), 204-210.

[39] R. P. Wool, Polymer interfaces: structure and strength, New York, Hanser, (1995).

[40] B. M. Malyshev, R. L. Salganik, The strength of adhesive joints using the theory of cracks, Int. J. Fract. Mech., 1 (1965), 114-128.

[41] H. Na, P. Chen, K.T. Wan, S.C. Wong, Q. Li, Z. Ma, Measurement of adhesion work of electropsun polymer membrane by shaft-loaded blister test. Langmuir, 28 (2012), 6677- 6683.

[42] K. T. Wan, Y.W. Mai, Fracture mechanics of a shaft-loaded blister of thin flexible membrane on rigid substrate, In. K. Fract., 74 (1995), 181-197.

[43] S.C. Wong, H. Na, P. Chen, Measurements of adhesion energy of electrospun polymer membranes using a shaft-loaded blister test, 13th Int. Conf. Fract. Mech, (2013), 1-7.

[44] W. R. Remington, E. K. Gladding, Equilibria in the dyeing of nylon with acid dyes, Journal of the American Chemical Society, 72 (1950), 2553-2559.

[45] S. Eshraghi, S. Das, Mechanical and microstructural properties of polycaprolactone scaffolds with one-dimensional, two-dimensional, and three-dimensional orthogonally oriented porous architectures produced by selective laser sintering, Acta Biomaterialia, 6 (2010), 2467-2476.

[46] M. Doi, S. F. Edwards, The Theory of Polymer Dynamics, Clarendon Press, Oxford (1986).

[47] T. S. Ellis, Polyamide-polyester blends: an estimation of the amide-ester interaction, Journal of Polymer Science: Part B Polymer Physics, 31 (1993), 1109-1125.

[48] G. C. Eastmond, H. Hocker, D. Klee, Biomedical Applications/ Polymer Blends, 149 Springer-Verlag Berlin, Heidelberg (1999).